

Free Vibration of Cross-ply Composite Plates by a High-Order Shear Deformable Finite Element

Mihir Chandra Manna^{1,*}, Mainak Manna²

¹Department of Aerospace Engineering and Applied Mechanics, Indian Institute of Engineering Science and Technology, Shibpur, Howrah, West Bengal, India

²Department of Computer Science and Technology, Indian Institute of Engineering Science and Technology, Shibpur, Howrah, West Bengal, India

Abstract

Free vibration analysis of composite rectangular plates with different thickness ratios, different boundary conditions and different aspect ratios has been investigated using a high-order shear flexible triangular plate element. The first order shear deformation theory (FOSDT) is used to include the effect of transverse shear deformation. The element has eighteen nodes on the sides and seven internal nodes. Element geometry is expressed in terms of three linear shape functions of area coordinates. The formulation is displacement type. The element has seventy-one degrees of freedom, which has been reduced to fifty-seven degrees of freedom by Guyan reduction scheme for the degrees of freedom associated with the internal nodes. Rotary inertia has been included in the consistent mass matrix. Numerical examples are presented to show the accuracy and convergence characteristics of the element.

Keywords: Shear deformation, Guyan reduction scheme, rotary inertia, consistent mass matrix

*Author for Correspondence E-mail: mcmbecdu@gmail.com

INTRODUCTION

Thick and thin isotropic and composite plates and shells have wide applications in ships, aircrafts, bridges, etc. A thorough study of their dynamic behavior and characteristics is essential to assess and use their full potentials. Different techniques like RBF-pseudo-spectral method, differential quadrature method, boundary characteristic orthogonal polynomials and pseudo-spectral method have been used in recent years [1–4]. More recently Kansa's nonsymmetric radial basis function (RBF) collocation method was applied by Ferreira for free vibration analysis of Timoshenko beams, Mindlin plates and composite plates [5, 6].

Other methods which have been very recently used for the aforementioned purposes are meshless method and discrete singular convolution (DSC) method [7, 8]. Shufrin et al. have investigated the free vibration of rectangular thick plates with variable thickness and different boundary conditions by using the extended Kantorovich method [9]. Kang et al.

have proposed a practical analytical method for the free vibration analysis of a simply supported rectangular plate with unidirectional arbitrary thickness variation [10]. But, since early sixties, Finite Element Method (FEM) has been proved to be more versatile tool in engineering fields [11, 12]. Plate bending is one of the first problems where the application of finite element was done in the early sixties. Initial attempts were made for bending and free vibration analyses with Kirchoff's hypothesis which showed a number of problems. These are mostly associated with the satisfaction of normal slope continuity on the interfaces between various elements.

Above-mentioned slope continuity problem has been eliminated by applying well-known Reissner-Mindlin's hypothesis for thick plates. In Reissner-Mindlin's hypothesis the transverse displacement (w) and rotations of normal (θ_x and θ_y) are expressed as independent field variables. A large number of published works on plate vibration are available as may be seen by inspection of the

excellent review articles by Leissa and Liew et al. and other comprehensive works by Yamada and Irie [13–21]. Also, a large number of triangular and quadrilateral finite elements were developed for analysis of thin as well as thick plates among which isoparametric elements became more popular [22]. Shear locking, stress extrapolation and spurious modes are some problems faced by these elements instead of having high legacy. To avoid the above-mentioned problems a number of thick plate bending elements have been proposed by many researchers [23–28]. Composite structures are weak in shear due to low shear modulus compared to extensional rigidity.

The present paper utilizes a triangular element with eighteen nodes equidistantly placed on the sides and seven nodes internal to it. The element has five degrees of freedom $(u, v, w, \theta_x, \theta_y)$ at the three nodes on the vertices (nodes 1, 7 and 13), at six side nodes nearer to mid-side nodes (nodes 3, 5, 9, 11, 15 and 17), three degrees of freedom (w, θ_x, θ_y) at three internal nodes (nodes 22–24), two degrees of freedom (θ_x, θ_y) at midpoint nodes (nodes 4, 10 and 16), two degrees of freedom (u, v) at centre node (node 25) and single degree of freedom (w) at nine nodes (nodes 2, 6, 8, 12, 14 and 18–21).

The element geometry is described by linear shape functions of area coordinates including corner nodes only. In the proposed element, the in-plane displacements (u, v) , the transverse displacement field (w) and both θ_x and θ_y are expressed by a third order polynomial, a fifth order polynomial and a fourth order polynomial, respectively.

The nodes are so placed on the sides and inside of the proposed element that the mass and rotary inertia for the internal nodes are negligible and well-known Guyan reduction scheme for the mass condensation is efficiently utilized to get highly accurate natural frequencies of rectangular composite plates under different boundary conditions [29].

FINITE ELEMENT FORMULATION

The formulation is based on the Reissner-Mindlin plate theory. In this theory it is assumed that the transverse deflection of the plate is small compared to the plate thickness and the normal to the plate mid surface which is taken as the reference plane remain straight but may not remain normal to the deformed mid surface. Twenty-five noded triangular element is used to develop the finite element analysis procedure. The element is shown in Figure 1.

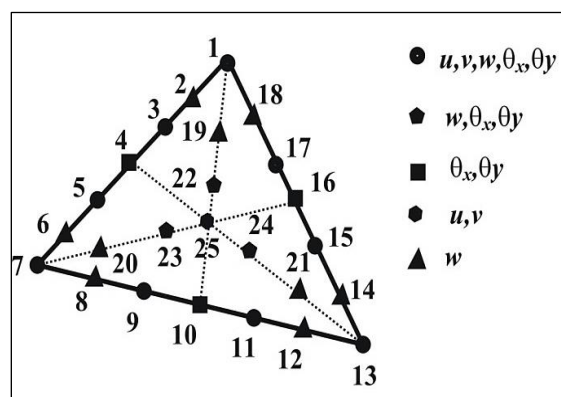


Fig. 1: Proposed Element.

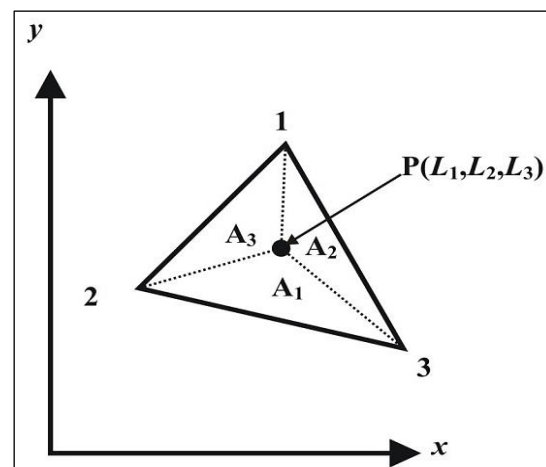


Fig. 2: Area Coordinates.

The element has five degrees of freedom $(u, v, w, \theta_x, \theta_y)$ at nodes 1, 3, 5, 7, 9, 11, 13, 15 and 17, three degrees of freedom (w, θ_x, θ_y) at nodes 22, 23 and 24, two degrees of freedom (θ_x, θ_y) at nodes 4, 10 and 16 and two degrees of freedom (u, v) at node 25 and single degree of freedom (w) at nodes 2, 6, 8, 12, 14 and 18–21.

The area coordinates (L_1, L_2, L_3) of the nodes are (1, 0, 0), (5/6, 1/6, 0), (2/3, 1/3, 0), (1/2, 1/2, 0), (1/3, 2/3, 0), (1/6, 5/6, 0), (0, 1, 0), (0, 5/6, 1/6), (0, 2/3, 1/3), (0, 1/2, 1/2), (0, 1/3, 2/3), (0, 1/6, 5/6), (0, 0, 1), (1/6, 0, 5/6), (1/3, 0, 2/3), (1/2, 0, 1/2), (2/3, 0, 1/3), (5/6, 0, 1/6), (2/3, 1/6, 1/6), (1/6, 2/3, 1/6), (1/6, 1/6, 2/3), (1/2, 1/4, 1/4), (1/4, 1/2, 1/4), (1/4, 1/4, 1/2) and (1/3, 1/3, 1/3).

The coordinates of any point P (Figure 2) within the element with respect to the global co-ordinate system are given by

$$\begin{aligned} x &= L_1x_1 + L_2x_2 + L_3x_3 \\ y &= L_1y_1 + L_2y_2 + L_3y_3 \end{aligned} \quad (1)$$

where, $L_i = A_i/A$, $i = 1, 2, 3$ and A is the area of the triangular element.

Again,

$$1 = L_1 + L_2 + L_3 \quad (2)$$

From Eqs. (1) and (2) we get,

$$L_i = (a_i + b_i x + c_i y) / 2A, \quad i = 1, 2, 3$$

where, $A = \frac{1}{2} [(x_2y_3 - x_3y_2) + (x_3y_1 - x_1y_3) + (x_1y_2 - x_2y_1)]$

$a_i = x_j y_k - x_k y_j$, $b_i = y_j - y_k$ and $c_i = x_k - x_j$ where the parameters i, j and k follow cyclic order of 1, 2 and 3.

The in-plane displacements (u, v), transverse displacement (w) and the rotations (θ_x and θ_y) of the normal are chosen as the complete third-order, fifth-order and fourth-order polynomials of area coordinates (L_1, L_2, L_3), respectively and are expressed as follows:

$$u = [\overline{L_{uv}}] \{\alpha_u\}, \quad v = [\overline{L_{uv}}] \{\alpha_v\}, \quad w = [\overline{L_w}] \{\alpha_w\}, \quad \theta_x = [\overline{L_{\theta_x}}] \{\alpha_{\theta_x}\} \quad \text{and} \quad \theta_y = [\overline{L_{\theta_y}}] \{\alpha_{\theta_y}\} \dots \quad (3)$$

where,

$$[\overline{L_{uv}}] = \{L_1^3 \quad L_2^3 \quad L_3^3 \quad L_1^2 L_2 \quad L_1 L_2^2 \quad L_2^2 L_3 \quad L_2 L_3^2 \quad L_3^2 L_1 \quad L_3 L_1^2 \quad L_1 L_2 L_3\}$$

$$[\overline{L_w}] = \{L_1^5 \quad L_2^5 \quad L_3^5 \quad L_1^4 L_2 \quad L_1 L_2^4 \quad L_2^4 L_3 \quad L_2 L_3^4 \quad L_3^4 L_1 \quad L_3 L_1^4\}$$

$$L_1^3 L_2^2 \quad L_1^2 L_2^3 \quad L_2^3 L_3^2 \quad L_2^2 L_3^3 \quad L_3^3 L_1^2 \quad L_3^2 L_1^3$$

$$L_1^3 L_2 L_3 \quad L_2^3 L_3 L_1 \quad L_3^3 L_1 L_2 \quad L_1^2 L_2^2 L_3 \quad L_2^2 L_3^2 L_1 \quad L_3^2 L_1^2 L_2\},$$

$$[\overline{L_{\theta_x}}] = [\overline{L_{\theta_y}}] = \{L_1^4 \quad L_2^4 \quad L_3^4 \quad L_1^3 L_2 \quad L_1 L_2^3 \quad L_2^3 L_3 \quad L_2 L_3^3 \quad L_3^3 L_1 \quad L_3 L_1^3 \quad L_1^2 L_2^2\}$$

$$L_2^2 L_3^2 \quad L_3^2 L_1^2 \quad L_1^2 L_2 L_3 \quad L_2^2 L_3 L_1 \quad L_3^2 L_1 L_2\},$$

$$\{\alpha_u\}^T = \{\alpha_1 \quad \alpha_2 \quad \alpha_3 \quad \alpha_4 \quad \alpha_5 \quad \alpha_6 \quad \alpha_7 \quad \alpha_8 \quad \alpha_9 \quad \alpha_{10}\},$$

$$\{\alpha_v\}^T = \{\alpha_{11} \quad \alpha_{12} \quad \alpha_{13} \quad \alpha_{14} \quad \alpha_{15} \quad \alpha_{16} \quad \alpha_{17} \quad \alpha_{18} \quad \alpha_{19} \quad \alpha_{20}\},$$

$$\{\alpha_w\}^T = \{\alpha_{21} \quad \alpha_{22} \quad \alpha_{23} \quad \alpha_{24} \quad \alpha_{25} \quad \alpha_{26} \quad \alpha_{27} \quad \alpha_{28} \quad \alpha_{29} \quad \alpha_{30} \quad \alpha_{31} \quad \alpha_{32} \quad \alpha_{33} \quad \alpha_{34} \\ \alpha_{35} \quad \alpha_{36} \quad \alpha_{37} \quad \alpha_{38} \quad \alpha_{39} \quad \alpha_{40} \quad \alpha_{41}\},$$

$$\{\alpha_{\theta_x}\}^T = \{\alpha_{42} \quad \alpha_{43} \quad \alpha_{44} \quad \alpha_{45} \quad \alpha_{46} \quad \alpha_{47} \quad \alpha_{48} \quad \alpha_{49} \quad \alpha_{50} \quad \alpha_{51} \quad \alpha_{52} \quad \alpha_{53} \quad \alpha_{54} \quad \alpha_{55} \quad \alpha_{56}\}, \quad \text{and}$$

$$\{\alpha_{\theta_y}\}^T = \{\alpha_{57} \quad \alpha_{58} \quad \alpha_{59} \quad \alpha_{60} \quad \alpha_{61} \quad \alpha_{62} \quad \alpha_{63} \quad \alpha_{64} \quad \alpha_{65} \quad \alpha_{66} \quad \alpha_{67} \quad \alpha_{68} \quad \alpha_{69} \quad \alpha_{70} \quad \alpha_{71}\}.$$

Putting the values of nodal in-plane displacements (u, v), transverse displacements (w), nodal normal rotations (θ_x and θ_y) and nodal area coordinates (L_1, L_2, L_3) in the above Eqs. (3) the values of α can be determined as follows:

$$\{\bar{u}\} = [\Psi_{uv}] \{\alpha_u\}, \{\bar{v}\} = [\Psi_{uv}] \{\alpha_v\},$$

$$\{\bar{w}\} = [\Psi_w] \{\alpha_w\}, \{\bar{\theta}_x\} = [\Psi_{\theta_x}] \{\alpha_{\theta_x}\}$$

and $\{\bar{\theta}_y\} = [\Psi_{\theta_y}] \{\alpha_{\theta_y}\}$ or,

$$\{\alpha_u\} = [\Psi_{uv}]^{-1} \{\bar{u}\}, \{\alpha_v\} = [\Psi_{uv}]^{-1} \{\bar{v}\}, \{\alpha_w\} = [\Psi_w]^{-1} \{\bar{w}\}, \{\alpha_{\theta_x}\} = [\Psi_{\theta_x}]^{-1} \{\bar{\theta}_x\}$$
 and

$$\{\alpha_{\theta_y}\} = [\Psi_{\theta_y}]^{-1} \{\bar{\theta}_y\}$$
 or $\{\alpha_u\}, \{\alpha_v\}, \{\alpha_w\}, \{\alpha_{\theta_x}\}$ and $\{\alpha_{\theta_y}\}$ may be assembled in a single matrix

form as

$$\{\alpha\} = [C] \{\delta\} \quad (4)$$

where,

$$[C] = \begin{bmatrix} [\Psi_{uv}]^{-1} & 0 & 0 & 0 & 0 \\ 0 & [\Psi_{uv}]^{-1} & 0 & 0 & 0 \\ 0 & 0 & [\Psi_w]^{-1} & 0 & 0 \\ 0 & 0 & 0 & [\Psi_{\theta_x}]^{-1} & 0 \\ 0 & 0 & 0 & 0 & [\Psi_{\theta_y}]^{-1} \end{bmatrix}$$

$$\{\alpha\}^T = \{\alpha_u\}^T \quad \{\alpha_v\}^T \quad \{\alpha_w\}^T \quad \{\alpha_{\theta_x}\}^T \quad \{\alpha_{\theta_y}\}^T, \quad \{\delta\}^T = \{\bar{u}\}^T \quad \{\bar{v}\}^T \quad \{\bar{w}\}^T \quad \{\bar{\theta}_x\}^T \quad \{\bar{\theta}_y\}^T,$$

$$\{\bar{u}\}^T = \{u_1 \quad u_3 \quad u_5 \quad u_7 \quad u_9 \quad u_{11} \quad u_{13} \quad u_{15} \quad u_{17} \quad u_{25}\},$$

$$\{\bar{v}\}^T = \{v_1 \quad v_3 \quad v_5 \quad v_7 \quad v_9 \quad v_{11} \quad v_{13} \quad v_{15} \quad v_{17} \quad v_{25}\},$$

$$\{\bar{w}\}^T = \{w_1 \quad w_2 \quad w_3 \quad w_5 \quad w_6 \quad w_7 \quad w_8 \quad w_9 \quad w_{11} \quad w_{12} \quad w_{13} \quad w_{14} \quad w_{15} \quad w_{17} \\ w_{18} \quad w_{19} \quad w_{20} \quad w_{21} \quad w_{22} \quad w_{23} \quad w_{24}\},$$

$$\{\bar{\theta}_x\}^T = \{\theta_{x1} \quad \theta_{x3} \quad \theta_{x4} \quad \theta_{x5} \quad \theta_{x7} \quad \theta_{x9} \quad \theta_{x10} \quad \theta_{x11} \quad \theta_{x13} \quad \theta_{x15} \quad \theta_{x16} \quad \theta_{x17} \quad \theta_{x22} \quad \theta_{x23} \quad \theta_{x24}\}$$

and

$$\{\bar{\theta}_y\}^T = \{\theta_{y1} \quad \theta_{y3} \quad \theta_{y4} \quad \theta_{y5} \quad \theta_{y7} \quad \theta_{y9} \quad \theta_{y10} \quad \theta_{y11} \quad \theta_{y13} \quad \theta_{y15} \quad \theta_{y16} \quad \theta_{y17} \quad \theta_{y22} \quad \theta_{y23} \quad \theta_{y24}\}$$

and hence, the field variables (u, v, w, θ_x and θ_y) can be expressed in the following manners:

$$\begin{Bmatrix} u \\ v \\ w \\ \theta_x \\ \theta_y \end{Bmatrix} = \begin{bmatrix} N_{uv} & N_0 & N_{00} & N_{000} & N_{000} \\ N_0 & N_{uv} & N_{00} & N_{000} & N_{000} \\ N_0 & N_0 & N_w & N_{000} & N_{000} \\ N_0 & N_0 & N_{00} & N_{\theta_{xy}} & N_{000} \\ N_0 & N_0 & N_{00} & N_{000} & N_{\theta_{xy}} \end{bmatrix} \{\delta\}$$

or,

$$\begin{Bmatrix} u \\ v \\ w \\ \theta_x \\ \theta_y \end{Bmatrix} = [N] \{\delta\} \quad (5)$$

where

$$N_{uv} = [\overline{L}_{uv}] [\Psi_{uv}]^{-1}, \quad N_w = [\overline{L}_w] [\Psi_w]^{-1},$$

$$N_{\theta_{xy}} = [\overline{L}_{\theta_{xy}}] [\Psi_{\theta_{xy}}]^{-1} \quad (6)$$

in which $[\Psi_{uv}]^{-1}$, $[\Psi_w]^{-1}$ and $[\Psi_{\theta_{xy}}]^{-1}$ are (10×10), (21×21) and (15×15) matrices, respectively, N_{uv} , N_w and $N_{\theta_{xy}}$ are row matrices containing 10, 21 and 15 elements, respectively and N_0 , N_{00} and N_{000} are null matrices of order (1×10), (1×21) and (1×15), respectively.

As rotations of the normal θ_x and θ_y are independent variables and they are not derivatives of w , the effect of shear deformation can be easily incorporated as:

$$\begin{Bmatrix} \phi_x \\ \phi_y \end{Bmatrix} = \begin{Bmatrix} w_{,x} - \theta_x \\ w_{,y} - \theta_y \end{Bmatrix} \quad (7)$$

where, ϕ_x and ϕ_y are average shear strain over the entire plate thickness and θ_x and θ_y are the total rotations of the normal.

The generalized stress-strain relationship may be expressed as

$$\{\sigma\} = [D] \{\varepsilon\} \quad (8)$$

In the above equation the generalized stress vector is

$$\{\sigma\}^T = \left\{ N_x \quad N_y \quad N_{xy} \quad M_x \quad M_y \quad M_{xy} \quad Q_x \quad Q_y \right\} \quad (9)$$

The generalized strain vector $\{\varepsilon\}$ in terms of displacement fields is

$$\{\varepsilon\}^T = \left\{ \varepsilon_x \quad \varepsilon_y \quad \varepsilon_{xy} \quad \kappa_x \quad \kappa_y \quad \kappa_{xy} \quad \varepsilon_{xz} \quad \varepsilon_{yz} \right\}$$

Or,

$$\{\varepsilon\}^T = \left\{ u_{,x} \quad v_{,y} \quad (u_{,y} + v_{,x}) \quad -\theta_{x,x} \quad -\theta_{y,y} \right. \\ \left. -(\theta_{x,y} + \theta_{y,x}) \quad w_{,x} - \theta_x \quad w_{,y} - \theta_y \right\} \quad (10)$$

and the rigidity matrix $[D]$ is given in details in [30].

With the help of Eqs. (4) and (5), the strain-displacement relationship may be expressed as

$$\{\varepsilon\} = [B]\{\delta\} \quad (11)$$

where, $[B]$ is a $(8 \times 7I)$ matrix and is given by

$$[B] = \begin{bmatrix} N_{uv,x} & N_0 & N_{00} & N_{000} & N_{000} \\ N_0 & N_{uv,y} & N_{00} & N_{000} & N_{000} \\ N_{uv,y} & N_{uv,x} & N_{00} & N_{000} & N_{000} \\ N_0 & N_0 & N_{00} & -N_{\theta_{xy,x}} & N_{000} \\ N_0 & N_0 & N_{00} & N_{000} & -N_{\theta_{xy,y}} \\ N_0 & N_0 & N_{00} & -N_{\theta_{xy,y}} & -N_{\theta_{xy,x}} \\ N_0 & N_0 & N_{w,x} & -N_{\theta_{xy}} & N_{000} \\ N_0 & N_0 & N_{w,y} & N_{000} & -N_{\theta_{xy}} \end{bmatrix} \quad (12)$$

Once the matrix $[B]$ is obtained, the element stiffness matrix $[K^e]$ can be easily derived with the help of the above equations using the virtual work technique and it may be expressed as

$$[K^e] = \int_A [B]^T [D][B] dA \\ = \int_A [B]^T [D][B] dx dy \quad (13)$$

In a similar manner, the consistent mass matrix of an element can be derived and it may be written with the help of Eq. (4) as

$$[M^e] = \int_A [N]^T [\bar{\rho}][N] dA \\ = \int_A [N]^T [\bar{\rho}][N] dx dy \quad (14)$$

where,

$$[\bar{\rho}] = \begin{bmatrix} \rho h & 0 & 0 & 0 & 0 \\ 0 & \rho h & 0 & 0 & 0 \\ 0 & 0 & \rho h & 0 & 0 \\ 0 & 0 & 0 & \frac{\rho h^3}{12} & 0 \\ 0 & 0 & 0 & 0 & \frac{\rho h^3}{12} \end{bmatrix}$$

and ρ is the overall density of the plate.

Stiffness and mass matrices obtained from Eqs. (13) and (14), respectively, using Gauss quadrature technique, are of the order of seventy-one by seventy-one. These matrices have been reduced to the required matrices $[K^{er}]$ and $[M^{er}]$ of the order of fifty-seven by fifty-seven by applying Guyan reduction scheme for global assembly [25]. The reduced element stiffness $[K^{er}]$ and element consistent mass matrices $[M^{er}]$ can be assembled into the following final form for free vibration equation of the plate:

$$[K]\{\delta\} - \omega^2 [M]\{\delta\} = 0 \quad (15)$$

The above equation has been solved by the simultaneous iterative technique of Corr and Jenning after substitution of boundary conditions to get first few frequencies for the lower modes of the plate [31].

NUMERICAL EXAMPLES

For all the examples, the warping factor (k) is assumed to be $\pi^2/12$. The geometry of the rectangular plate is shown in Figure 3. The boundary conditions of the plate with clamped edge ($x=0$), simply supported edge ($x=a$), clamped edge ($y=0$) and free edge ($y=b$) are symbolized as CSCF. The eigenvalues obtained in the present investigation have been expressed in the non-dimensional form which is defined by the parameter $\lambda_i = (\omega_i b^2 / \pi^2) \sqrt{(\rho t / D)}$. Several case studies have been investigated for symmetric composite rectangular plates with different thickness ratios ($t/b=0.001, 0.05, 0.1, 0.15$ and 0.2), different aspect ratios ($a/b=1.0$ and 2.0) and different combinations of simply supported (S), clamped (C) and free (F) boundary conditions. The material properties for all the layers of the laminates are identical and are taken as $E_{11}/E_{22}=40; G_{23} = 0.5E_{22}; G_{12} = G_{31} = 0.6E_{22}; \nu_{12} = 0.25; \nu_{21} = 0.00625$.

Convergence studies have been carried out for three-ply laminates with stacking sequence $(0^\circ, 90^\circ, 0^\circ)$ for two selected boundary conditions, namely SSSS and CFFF. The

laminates are analysed with rotary inertia with thickness ratios ($t/b=0.001$ and 0.2) and different aspect ratios ($a/b=1.0$ and 2.0). The results obtained for different mesh divisions are shown in Table 1 along with Liew [32].

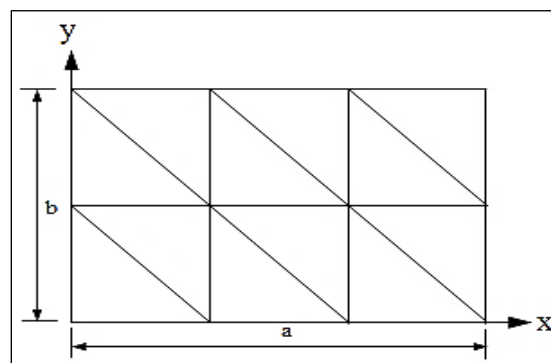


Fig. 3: Rectangular Plate (Mesh 3x2).

Table 1 shows that the results obtained from the present analysis are very close to those by Liew [32]. To see the effect of thickness-to-length ratio (t/b) on the fundamental frequency parameters obtained by the present formulation, a simply supported four-ply symmetric laminates with stacking sequence $(0^\circ, 90^\circ, 90^\circ, 0^\circ)$ are presented in Table 2 with those by Ferreira and Fasshauer, Liew and Reddy and Phan [1, 32, 33]. From Table 2, it has been observed that the present results are in good agreement with the results obtained by Ferreira and Fasshauer, Liew and Reddy and Phan [1, 32, 33]. To study the efficiency of the present finite element formulation on the effect of other boundary conditions, thickness ratios, stacking sequences and the aspect ratios, the problem of free vibration analysis of composite rectangular plates having different lamina layers is considered as follows: The laminate consists of layers of equal thickness. The rectangular plate is analyzed numerically with different boundary conditions, namely CCCC, SSSC, SSFF and CCFF for three-ply laminates with stacking sequence $(0^\circ, 90^\circ, 0^\circ)$ with different thickness ratios ($t/b=0.001$ and 0.2) and aspect ratios ($a/b=1.0$ and 2.0). The results are presented in Tables 3 and 4 with those by Ferreira and Fasshauer and Liew [1, 32]. Another problem of five-ply laminate plates with stacking sequence $(0^\circ, 90^\circ, 0^\circ, 90^\circ, 0^\circ)$ for CCCC and

SSCC boundary conditions is considered. The results obtained are depicted in Table 5 along with the results obtained Ferreira and Fasshauer and Liew [1, 32]. Lastly the problem of eight-ply laminated plates with stacking sequence $\{(0^\circ, 90^\circ, 0^\circ, 90^\circ)_2\}$ for SFSF and CFCF boundary conditions has been considered. The results are tabulated in

Table 6 along with Liew [32]. From Tables 2–6, it has been seen that the present analysis give the non-dimensional frequency parameters very close to the results obtained by Ferreira and Fasshauer and Liew for very thin as well thick laminated plates for different stacking sequences, different aspect ratios and different boundary conditions.

Table 1: Convergence Study of Frequency Parameters $[\lambda=(\omega b^2/\pi^2)\sqrt{(\rho h/D_0)}]$ for Three-ply $(0^\circ, 90^\circ, 0^\circ)$ Simply Supported and Clamped Rectangular Laminate Plates.

Boundary Condition	a/b	t/b	Source	Mode sequences					
				1	2	3	4	5	6
SSSS	1	0.001	PS-2	6.6254	9.4711	16.4827	25.1359	26.8820	27.2144
			PS-4	6.6252	9.4472	16.2064	25.1155	26.4997	26.6724
			PS-6	6.6252	9.4471	16.2053	25.1150	26.4986	26.6580
			PS-8	6.6252	9.4471	16.2052	25.1149	26.4984	26.6575
			[32]	6.6252	9.4470	16.2051	25.1146	26.4982	26.6572
			PS-4	3.6073	5.8231	7.5125	8.8690	9.3537	11.5927
			PS-8	3.5972	5.7827	7.4263	8.7342	9.1990	11.3090
			PS-12	3.5954	5.7752	7.4102	8.7085	9.1692	11.2539
	2	0.001	PS-2	2.3619	6.6329	6.6739	9.6370	14.3567	14.5166
			PS-4	2.3618	6.6253	6.6646	9.4474	14.2877	14.3854
			PS-6	2.3618	6.6252	6.6646	9.4471	14.2871	14.3847
			PS-8	2.3618	6.6252	6.6645	9.4471	14.2871	14.3847
			[32]	2.3618	6.6252	6.6845	9.4470	14.2869	14.3846
			PS-4	1.9430	3.6172	4.9323	5.5666	5.8621	7.2851
			PS-8	1.9402	3.5997	4.8899	5.5062	5.7929	7.1626
			PS-12	1.9397	3.5965	4.8819	5.4948	5.7797	7.1380
CFFF	1	0.001	PS-2	2.2119	2.4860	4.7424	10.5340	13.8598	14.1730
			PS-4	2.2119	2.4879	4.7497	10.5345	13.8599	14.1798
			PS-6	2.2119	2.4884	4.7512	10.5356	13.8599	14.1807
			PS-8	2.2119	2.4886	4.7518	10.5361	13.8599	14.1811
			[32]	2.2119	2.4890	4.7530	10.5370	13.8598	14.1817
			PS-4	1.4453	1.5458	3.4765	4.7160	4.8924	6.0430
			PS-8	1.4446	1.5450	3.4684	4.6940	4.8685	6.0011
			PS-12	1.4445	1.5448	3.4668	4.6898	4.8639	5.9930
	2	0.001	PS-2	0.5529	0.7863	3.4634	3.7437	3.7768	5.8191
			PS-4	0.5529	0.7876	3.4635	3.7457	3.7800	5.8332
			PS-6	0.5529	0.7879	3.4635	3.7460	3.7809	5.8364
			PS-8	0.5529	0.7881	3.4635	3.7462	3.7812	5.8376
			[32]	0.5529	0.7882	3.4635	3.7464	3.7819	5.8401
			PS-4	0.4796	0.6215	1.9428	2.1307	3.1394	3.8997
			PS-8	0.4795	0.6214	1.9400	2.1271	3.1296	3.8808
			PS-12	0.4795	0.6214	1.9394	2.1264	3.1277	3.8770
0.200	0.001	PS-16	0.4795	0.6214	1.9393	2.1262	3.1270	3.8757	
		[32]	0.4795	0.6214	1.9390	2.1259	3.1260	3.8739	

PS-8 Present Study with rotary inertia with mesh division (8x8).

Table 2: Effect of Thickness-to-length Ratio on the Fundamental Frequency Parameters $[\lambda=(\omega b^2/\pi^2)\sqrt{(\rho h/D_0)}]$ for a Simply Supported Square Four-ply ($0^\circ, 90^\circ, 0^\circ, 90^\circ$) Laminate Plates.

t/b	0.01	0.02	0.04	0.05	0.08	0.10	0.20	0.25	0.50
PS-2	6.6088	6.5547	6.3496	6.2091	5.7035	5.3435	3.8534	3.3425	1.9674
PS-4	6.6063	6.5495	6.3375	6.1931	5.6762	5.3100	3.8075	3.2964	1.9309
PS-6	6.6061	6.5488	6.3357	6.1905	5.6714	5.3039	3.7988	3.2877	1.9240
PS-8	6.6060	6.5486	6.3351	6.1896	5.6697	5.3018	3.7958	3.2847	1.9215
PS-10	6.6060	6.5486	6.3348	6.1892	5.6689	5.3008	3.7944	3.2833	1.9203
PS-12	6.6060	6.5485	6.3347	6.1891	5.6685	5.3003	3.7936	3.2825	1.9197
PS-14	6.6060	6.5485	6.3347	6.1890	5.6683	5.3000	3.7931	3.2820	1.9193
PS-16	6.6060	6.5485	6.3347	6.1889	5.6683	5.3000	3.7928	3.2817	1.9191
PS-18	6.6060	6.5485	6.3347	6.1889	5.6683	5.3000	3.7926	3.2815	1.9189
PS-20	6.6060	6.5485	6.3347	6.1889	5.6683	5.3000	3.7925	3.2814	1.9188
[1]	6.6012	6.5438	6.3300	6.1844	5.6641	5.2960	3.7903	3.2796	1.9180
[32]	6.606	6.549	6.338	6.193	5.677	5.311	3.807	3.295	1.929
[33]	6.578	6.475	6.330	6.196	5.708	5.355	3.854	3.331	1.956

Table 3: Frequency Parameters $[\lambda=(\omega b^2/\pi^2)\sqrt{(\rho h/D_0)}]$ for Three-ply Laminated Plates ($0^\circ, 90^\circ, 0^\circ$) for CCCC and SSSC Boundary Conditions.

Boundary Condition	a/b	t/b	Source	Mode sequences						
				1	2	3	4	5	6	
CCCC	1	0.001	PS-8	14.6656	17.6139	24.5118	35.5326	39.1586	40.7695	
			[1]	14.6918	18.4741	26.9611	37.6121	39.3560	40.9241	
			[32]	14.666	17.614	24.511	35.532	39.157	40.768	
		0.200	PS-16	4.4482	6.6473	7.7079	9.1991	9.7546	11.4277	
			[1]	4.4465	6.6420	7.6995	9.1848	9.7377	11.3990	
			[32]	4.447	6.642	7.700	9.185	9.738	11.399	
	2	0.001	PS-8	5.1051	10.5266	10.5829	14.3244	19.5679	19.7013	
			[1]	5.0970	10.4052	10.6097	14.3575	18.9482	19.7608	
			[32]	5.105	10.527	10.583	14.324	19.567	19.701	
		0.200	PS-16	3.0463	4.2509	5.7978	5.9112	6.5441	7.7029	
			[1]	3.0452	4.2481	5.7916	5.9042	6.5347	7.6885	
			[32]	3.045	4.248	5.792	5.905	6.535	7.688	
SSSC	1	0.001	PS-8	7.3961	12.1439	20.8411	25.3652	27.6717	33.0324	
			[32]	7.396	12.144	20.841	25.365	27.671	33.032	
			PS-16	4.1382	6.4792	7.6728	9.1732	9.6597	11.4048	
		[32]	4.137	6.474	7.664	9.159	9.642	11.377		
		2	0.001	PS-8	3.9840	7.3961	10.0616	12.1446	14.6894	17.9147
				[32]	3.984	7.396	10.061	12.144	14.688	17.912
	PS-16			2.8407	4.1392	5.7131	5.8551	6.4838	7.6790	
	[32]	2.840	4.137	5.707	5.848	6.474	7.664			

Table 4: Frequency Parameters $[\lambda=(\omega b^2/\pi^2)\sqrt{(\rho h/D_0)}]$ for Three-ply Laminated Plates ($0^\circ, 90^\circ, 0^\circ$) for SSFF and CCFB Boundary Conditions.

Boundary Condition	a/b	t/b	Source	Mode sequences						
				1	2	3	4	5	6	
SSFF	1	0.001	PS-8	6.2079	6.4356	7.9749	12.7521	21.3460	24.8317	
			[32]	6.208	6.436	7.975	12.752	21.346	24.831	
		0.200	PS-16	3.2134	3.3116	4.6208	7.2022	7.2793	7.6063	
			[32]	3.213	3.311	4.619	7.195	7.272	7.599	
	2	0.001	PS-8	1.5545	1.7723	4.2594	6.2101	6.4357	7.9777	
			[32]	1.552	1.770	4.257	6.208	6.436	7.975	
		0.200	PS-16	1.1952	1.3307	3.2138	3.3121	3.4057	4.6222	
			[32]	1.195	1.331	3.213	3.311	3.405	4.619	
CCFB	1	0.001	PS-8	14.0725	14.1989	15.0363	18.1352	25.0385	36.0012	
			[32]	14.072	14.199	15.037	18.136	25.039	36.000	
			0.200	PS-16	3.6370	3.6724	4.8094	7.2419	7.3160	7.6887
				[32]	3.636	3.672	4.807	7.235	7.309	7.681
	2	0.001	PS-8	3.5189	3.6456	5.3700	9.6990	9.8699	10.8000	
			[32]	3.518	3.644	5.369	9.698	9.869	10.799	
			0.200	PS-16	1.6619	1.7047	3.3673	3.4444	3.5155	4.6931
				[32]	1.662	1.704	3.366	3.443	3.514	4.690

Table 5: Frequency Parameters $[\lambda=(\omega b^2/\pi^2)\sqrt{(\rho h/D_0)}]$ for Five-ply Laminated Plates ($0^\circ, 90^\circ, 0^\circ, 90^\circ, 0^\circ$) for CCCC and SSCC Boundary Conditions.

Boundary Condition	a/b	t/b	Source	Mode sequences						
				1	2	3	4	5	6	
CCCC	1	0.001	PS-8	14.6671	23.1591	36.1648	39.5823	40.7785	52.4086	
			[1]	14.4337	18.7244	35.8179	40.9718	40.9718	52.5993	
			[32]	14.667	23.159	36.164	39.582	40.777	52.404	
		0.200	PS-16	4.8432	7.4820	7.8679	9.7445	10.9468	11.4868	
			[1]	4.8279	7.5339	7.7699	9.7082	11.0603	11.2888	
			[32]	4.841	7.474	7.859	9.728	10.923	11.457	
	2	0.001	PS-8	7.6278	11.3501	18.8367	19.2392	21.1953	26.2397	
			[1]	7.5611	11.1165	17.4333	19.2374	21.3109	24.2316	
			[32]	7.628	11.350	18.836	19.239	21.195	26.239	
		0.200	PS-16	3.6270	4.6392	6.1545	6.7584	7.3700	7.8590	
			[1]	3.6566	4.6327	6.1015	6.8399	7.4233	7.7551	
			[32]	3.625	4.636	6.147	6.748	7.357	7.843	
SSCC	1	0.001	PS-8	9.0725	20.0280	23.9009	30.3271	37.7886	44.6450	
			[32]	9.072	20.028	23.901	30.327	37.787	44.643	
			0.200	PS-16	4.5115	7.2917	7.8206	9.7086	10.8256	11.4571
				[32]	4.510	7.285	7.812	9.691	10.801	11.429
	2	0.001	PS-8	7.0510	9.0725	14.7085	19.0029	20.0285	23.3996	
			[32]	7.051	9.072	14.708	19.003	20.028	23.398	
			0.200	PS-16	3.4438	4.5128	6.0857	6.6726	7.2975	7.8277
				[32]	3.442	4.510	6.078	6.663	7.285	7.812

Table 6: Frequency Parameters [$\lambda = (\omega b^2 / \pi^2) \sqrt{(\rho h / D_0)}$] for Eight-ply Laminated Plates $\{(0^\circ, 90^\circ, 0^\circ, 90^\circ)_2\}$ for SFSF and CFCF Boundary Conditions.

Boundary Condition	a/b	t/b	Source	Mode sequences						
				1	2	3	4	5	6	
SFSF	1	0.001	PS-8	0.4657	5.8411	8.3537	10.8837	18.5189	21.3252	
			[32]	0.466	5.841	8.354	10.886	18.519	21.328	
	0.200	PS-16	0.4300	3.9257	4.4945	6.0396	8.0847	8.5712		
		[32]	0.430	3.925	4.493	6.035	8.075	8.560		
		2	0.001	PS-8	0.2410	2.1759	5.7142	6.4020	6.7706	9.4371
				[32]	0.232	2.175	5.714	6.402	6.771	9.438
0.200	PS-16	0.2192	1.6994	3.7658	3.8588	4.2862	5.4760			
	[32]	0.219	1.699	3.764	3.857	4.284	5.471			
	CFCF	1	0.001	PS-8	2.3901	8.5219	11.9813	15.1706	22.9460	26.7701
				[32]	2.390	8.522	11.982	15.174	22.946	26.774
0.200		PS-16	1.7297	4.2590	4.6278	6.1538	8.2950	8.7338		
		[32]	1.730	4.258	4.626	6.150	8.284	8.722		
		2	0.001	PS-8	1.4214	3.3478	8.1671	8.4574	8.9929	12.2275
				[32]	1.421	3.347	8.167	8.458	8.994	12.229
0.200	PS-16	1.1649	2.1397	3.9957	4.0498	4.4936	5.6447			
	[32]	1.165	2.139	3.994	4.048	4.491	5.639			

CONCLUSIONS

A twenty-five node triangular shear flexible plate bending element with seventy-one degrees of freedom has been utilized to investigate the free vibration of laminated composite rectangular plates with different thickness ratios, aspect ratios, stacking sequences and boundary conditions. The degrees of freedom associated with the seven internal nodes are condensed by Guyan reduction scheme to get the reduced element stiffness and mass matrices of the order of fifty-seven by fifty-seven. A comparative study of present results with those of earlier investigators shows the rapid convergence characteristics and accuracy of the present element for very thin to thick plates. It can also be concluded that due to increase of node numbers on the edges of the proposed element the mass and rotary inertia distribution at different nodes are such that the mass as well as rotary inertia associated with the internal nodes are negligible compared to those with the nodes on the edges. This helps the application of Guyan reduction scheme to this element efficiently and accurately.

REFERENCES

1. Ferreira AJM, Fasshauer GE: Analysis of natural frequencies of composite plates by an RBF-pseudospectral method. *Compos Struct.* 2007; 79(2): 202–210p.
2. Liew KM, Han JB, Xiao ZM: Vibration analysis of circular plates using differential quadrature method. *J Sound Vib.* 1997; 205(5): 617–630p.
3. Liew KM, Hung KC, Lim MK: Vibration of Mindlin plates using boundary characteristic orthogonal polynomials. *J Sound Vib.* 1995; 182(1): 77–90p.
4. Lee J, Schultz WW: Eigenvalue analysis of Timoshenko beams and axisymmetric Mindlin plates by the pseudospectral method. *J Sound Vib.* 2004; 269: 609–621p.
5. Ferreira AJM: Free vibration analysis of Timoshenko beams and Mindlin plates by radial basis functions. *Int J Comput Methods.* 2005; 2(1): 15–31p.
6. Ferreira AJM: Analysis of composite plates using a layerwise deformation theory and multiquadrics discretization. *Mech Adv Mater Struct.* 2005; 12(2): 99–112p.
7. Ferreira AJM, Batra RC, Roque CMC, *et al.*: Static analysis of functionally graded plates using third-order shear deformation theory and a meshless method. *Compos Struct.* 2005; 69: 449–457p.
8. Omer Cvalek: Free vibration analysis of symmetrically laminated composite plates

- with first-order shear deformation theory (FSDT) by discrete singular convolution method. *Finite Elem Anal Des.* 2008; 44: 725–731p.
9. Shufrin I, Eisenberger M: Vibration of shear deformable plates with variable thickness – first-order and higher-order analyses. *J Sound Vib.* 2006; 290: 465–489p.
 10. Kang SW, Kim S-H: Variation analysis of simply supported rectangular plates with unidirectionally, arbitrarily varying thickness. *J Sound Vib.* 2008; 312: 551–562p.
 11. Zienkiewicz OC, Taylor RL: *The Finite Element Methods* (Two Volumes), New York: McGraw Hill, 1988.
 12. Cook RD, Malkus DS, Plesha ME: *Concepts and Applications of Finite Element Analysis*, John Wiley & Sons, 1989.
 13. Liessa AW: *Vibration of Plates* (NASA SP – 160). Washington, D. C.: U. S. Government Printing office, 1969.
 14. Liessa AW: Recent research in plate vibrations, 1973 – 1976: classical theory. *Shock Vib Digest*, 1977; 9(10): 13–24p.
 15. Liessa AW: Recent research in plate vibrations, 1973 – 1976: complicating effects. *Shock Vib Digest.* 1977; 9(11): 21–35p.
 16. Liessa AW: Plate vibration research, 1976 – 1980: classical theory. *Shock Vib Digest.* 1981; 13(9): 11–22p.
 17. Liessa AW: Plate vibration research, 1976 – 1980: complicating effects. *Shock Vib Digest.* 1981; 13(10): 19–36p.
 18. Liessa AW: Plate vibration research, 1981 – 1985, part I: Classical theory. *Shock Vib Digest.* 1987; 19(2): 11–18p.
 19. Liessa AW: Plate vibration research, 1981–1985, part II: Complicating effects. *Shock Vib Digest.* 1987; 19(3): 10–24p.
 20. Liew KM, Xiang Y, Kitipornchai S: Research on thick plate vibration: A literature survey. *J Sound Vib.* 1995; 180(1): 163–176p.
 21. Yamada GY, Irie T: Plate vibration research in Japan. *Appl Mech Rev.* 1987; 40: 879–892p.
 22. Hrabok MM, Hrudey TM: A review and catalogue of plate bending finite elements. *Comp Struct.* 1984; 19(3): 479–495p.
 23. Petrolito J: A modified ACM element for tick plate analysis. *Comp Struct.* 1989; 32: 1303–1309p.
 24. Yuan FG, Miller RE: A cubic triangular finite element for flat plates with shear. *Int J Num Method Eng.* 1989; 28: 109–126p.
 25. Brasile S: An isotropic assumed stress triangular element for Reissner-Mindlin plate-bending problem. *Int J Num Methods Engg.* 2008; 74: 971–995p.
 26. Choo YS, Choi N, Lee BC: A new hybrid-Trefftz triangular and quadrilateral elements. *Appl Math Modell.* 2010; 34: 14–23p.
 27. Cai YC, Tian LG, Atluri SN: A simple locking-free discrete shear triangular plate element. *Comp Model Engg Sci.* 2011; 77: 221–238p.
 28. Zhuang XY, Huang RQ, Zhu HH, et al. A new and simple locking-free triangular thick plate element using independent shear degrees of freedom. *Finite Elem Anal Des.* 2013; 75: 1–7p.
 29. Guyan RJ: Reduction of stiffness and mass matrices. *AIAA J.* 1965; 3(2): 380p.
 30. Jones RM: *Mechanics of Composite Materials*, 2nd Edn. Taylor & Francis, 1999.
 31. Corr RB, Jennings A: A simultaneous iteration algorithm for symmetric eigenvalue problems. *Int J Num Method Eng.* 1976; 10: 647–663p.
 32. Liew KM: Solving the variation thick symmetric laminates by Reissner/Mindlin plate theory and p-Ritz method. *J Sound Vib.* 1996; 198(3): 343–360p.
 33. Reddy JN, Phan ND: Stability and vibration of isotropic, orthotropic and laminated plates according to a higher-order deformation theory. *J Sound Vib.* 1985; 98(2): 165–170p.

Cite this Article

Mihir Chandra Manna, Mainak Manna. Free Vibration of Cross-ply Composite Plates by A High-Order Shear Deformable Finite Element. *Research & Reviews: Journal of Physics.* 2016; 5(3): 36–47p.